Molecular Crystals and Liquid Crystals Science and Technology. Section A. Molecular Crystals and Liquid Crystals

Publication details, including instructions for authors and subscription information:
http://www.tandfonline.com/loi/gmcl19

Photoenhanced Conductivity in Organic Crystals

Jan Godlewski [a] , Jan Kalinowski [b c] & Piergiulio Di Marco [b]

[a] Department of Molecular Physics, Technical University of Gda[ngrave]sk, 80-952, Gda[ngrave]sk, Poland

[b] Istituto di Fotochimica e Radiazioni d'Alta Energia, CNR, 40126, Boiogna, Italy

[c] Department of Molecular Physics, Technical University of Gdansk, 80-952, Gdansk, Poland

Version of record first published: 24 Sep 2006.

To cite this article: Jan Godlewski , Jan Kalinowski & Piergiulio Di Marco (1993): Photoenhanced Conductivity in Organic Crystals, Molecular Crystals and Liquid Crystals Science and Technology. Section A. Molecular Crystals and Liquid Crystals, 228:1, 61-68

To link to this article: http://dx.doi.org/10.1080/10587259308032144

Mol. Cryst. Liq. Cryst. 1993, Vol. 228, pp. 61–68
Reprints available directly from the publisher
Photocopying permitted by license only

Printed in the United States of America

PHOTOENHANCED CONDUCTIVITY IN ORGANIC CRYSTALS*

JAN GODLEWSKI
Department of Molecular Physics, Technical University of Gdańsk, 80-952 Gdańsk, Poland.

JAN KALINOWSKI** and PIERGIULIO DI MARCO
Istituto di Fotochimica e Radiazioni d'Alta Energia, CNR, 40126 Bologna, Italy

Abstract Macrotrap model for charge carrier trapping is applied to describe photo-enhanced currents in anthracene-like crystals. The currents are due to the interaction between triplet excitons and charge carriers trapped in spatially extended trapping domains (macrotraps). The model allows to selfconsistency explain experimental voltage and light intensity dependences of the photo-enhanced conductivity measured in anthracene crystals.

INTRODUCTION

The term "photo-enhanced conductivity" describes photoconductivity in the space-charge-limited regime due to optical excitation of charge carriers out of carrier traps.[1] A theoretical description of single carrier photo-enhanced currents (PEC) was achieved by applying the occupation statistics of point (dimensionless) traps in the presence of optical excitation.[2-4] This description fails to explain experimentally observed non-quadratic dependence of PEC on applied voltage. In the present paper we show that the triplet exciton interaction with charge carriers localized in the electric field-modified spatially extended trapping domains allows to understand such a behaviour of PEC.

EXPERIMENTAL RESULTS

The principle features of PEC in organic crystals are illustrated using as an example a model crystal of anthracene ($C_{14}H_{10}$). Solution-grown anthracene single crystals with well developed (ab) crystallographic planes are typically 50 - 200 μm thick, and for electrical measurements they are overcoated with (semitransparent) CuJ electrodes ~ 0.1 cm^2 in area.

Figure 1 shows the field (F) dependence of the dark and photoenhanced current in a log-log scale for three of over 10 examined anthracene crystals. While the dark space-charge-limited current (SCLC) follows a power law $j_{dark} \sim F^n$ with $n >> 1$, the field dependence of PEC is, in general, more complex,

* The work supported in part by the Polish State Research Council (KBN) under project nr. 204599101 for the period 1992-1994.

** On leave from Department of Molecular Physics, Technical University of Gdańsk, 80-952 Gdańsk, Poland.

and only in one case can be approximated by a power function $j \sim F^m$ (m=2) within a low-field region $F < 2x10^4$ V/cm.

For high fields ($F > 2x10^4$ V/cm) the PEC approach the dark current in the examined crystals.

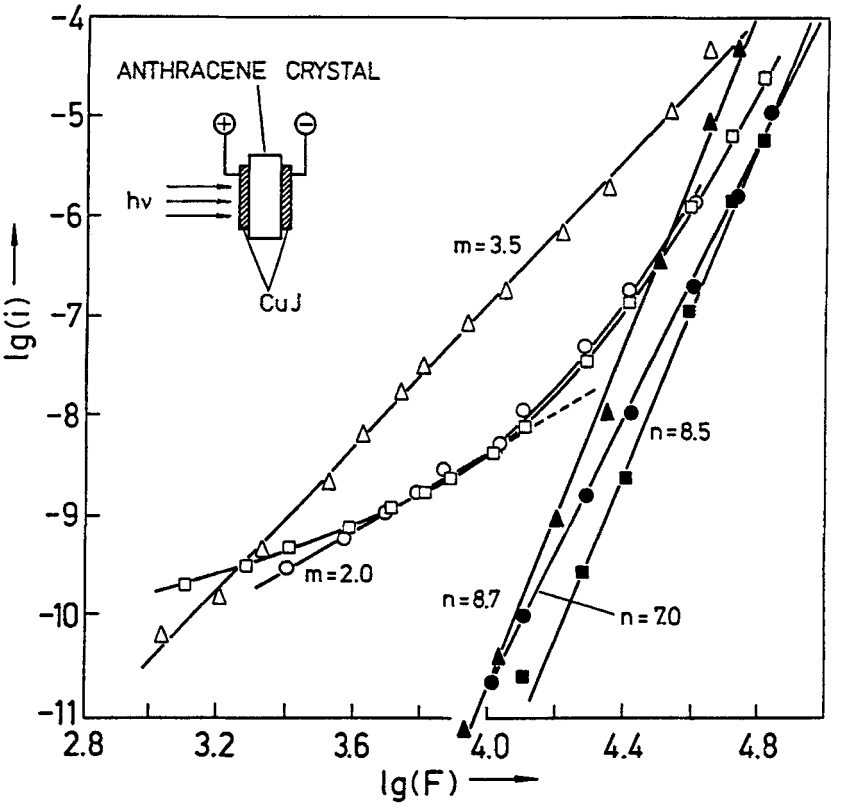

FIGURE 1 Field dependences of the dark (full figure points) and photo-enhanced (open figure points) currents for three different anthracene crystals of thickness d=78 μm (squares); d=78 μm (circles; the crystal different from the first one); d = 94 μm (triangles). Light intensity $I_0 \approx 10^{15}$ photons/cm^{2}s. The spectral region of the exciting light ($410 < \lambda < 450$ nm) preselected to obtain approximately homogeneous distribution of excitons throughout entire thickness of the crystals (the penetration depth of the major part of the light flux exceeds each crystal thickness).

THEORETICAL CONSIDERATIONS

We assume that PEC in anthracene-like crystals, proceed by triplet exciton-trapped charge carrier interaction. This is because the triplet exciton concentration, [T], resulted from directly excited singlets by 5% intersystem crossing, is about a factor of 10^3 greater than that of singlets, [S], due to the relation

between their lifetimes ($\tau_{TO} \approx 10$ ms, $\tau_{SO} \approx 10$ ns). Since the interaction with trapped charge carriers of concentration n_t leads to an additional decay channel for triplet excitons, a kinetic equation for them in steady-state conditions can be written as follows:

$$\frac{d[T]}{dT} = \kappa\tau_{SO}k_{ISC}I_O - \frac{[T]}{\tau_{TO}} - k_{Th}n_t[T] = 0 \quad . \tag{1}$$

Here κ is the absorption coefficient of weakly-absorbed light, k_{ISC} is the intersystem crossing rate constant, and k_{Th} stands for the second order rate constant for the triplet exciton-trapped carrier interaction.

From (1)

$$[T] = \frac{\kappa I_O \tau_{SO}\tau_{TO}k_{ISC}}{1 + k_{Th}n_t\tau_{TO}}, \tag{2}$$

and two limiting cases can be distinguished:

$$[T] \approx \kappa\tau_{SO}\tau_{TO}k_{ISC}I_O \quad \text{for} \quad k_{Th}n_t\tau_{TO} \ll 1 \tag{3a}$$

and

$$[T] \approx \kappa\tau_{SO}k_{ISC}I_O / \kappa_{Th}n_t \quad \text{for} \quad k_{Th}n_t\tau_{TO} \gg 1 \; . \tag{3b}$$

Since

$$n_{tot} \approx (3/2)(\epsilon\epsilon_o U)/ed^2 \tag{4}$$

is proportional to the applied voltage (U) one would expect the (3a) approximation to be obeyed in the low-field region, and (3b) to be obeyed in the high-field region for a crystal of given thickness, d, characterized by the dielectric constant ϵ. However, at the same n_t, different cases can be realized dependent on the product $k_{Th}\tau_{TO}$.

Therefore, conditions (3) do not form good criteria for the field regional division. The PEC under trapping by a discrete set of traps is given by[2]

$$j_{PEC} \approx \theta\epsilon\epsilon_o\mu U^2/d^3 \quad , \tag{5}$$

where μ is the carrier mobility, and θ is the ratio of free (n_f) to total (n_{tot}) carrier concentration, which, in general, is a complicated function of U, d, x-position in the crystal, I_o, and other parameters. If $n_f \ll n_t = n_{tot}$, θ can be obtained from the detailed balance relationship

$$\{(D/r_o^2)\exp[-(E_t - \Delta E)/kT] + \eta k_{Th}[T]\}n_t = n_f 4\pi r_o D N_o \quad , \tag{6}$$

where D is the diffusion coefficient of charge carriers, N_o is the concentration and r_o the radius of trapping centers (see Fig. 2). The carriers are assumed to be captured by spatially extended spherical symmetry domains (macrotraps),[5-8] when the capture radius, r_o, exceeds the mean free path, λ, of the carrier. The steady-state diffusion-limited lifetime of the carriers is then given by[9]

$$\tau_c = (4\pi D N_0 r_o)^{-1} \quad . \tag{7}$$

We note that the first term in the left-hand curly bracket expression describes thermal detrapping and the second one optical detrapping of charge carriers with efficiency, η, dependent on the carrier relaxation process.

In general, the field lowers the energy barrier for the macrotrap, $E_t - \Delta E$, increases θ, and therefore causes j_{PEC} to increase more steeply than U^2. As has been shown previously[5,6]

$$\Delta E \approx eFr_o \tag{8}$$

for low fields, and

$$\Delta E \approx \frac{3kT}{\sigma} \ln\left(\frac{2.7\sigma eFr_o}{3kT}\right) \tag{9}$$

for high fields applied to the crystal. There are several limiting situations for which exact results can be obtained for the j_{PEC} (F) function shape. First, we consider the real PEC, for which

$$\eta k_{Th}[T] \gg (D/r_o^2)\exp[-(E_t - \Delta E)/kT] \quad . \tag{10}$$

Two field regions can be distinguished according to (8) and (9):

Low-field region (LFR)

(a) $k_{Th} n_t \tau_{TO} \ll 1$.

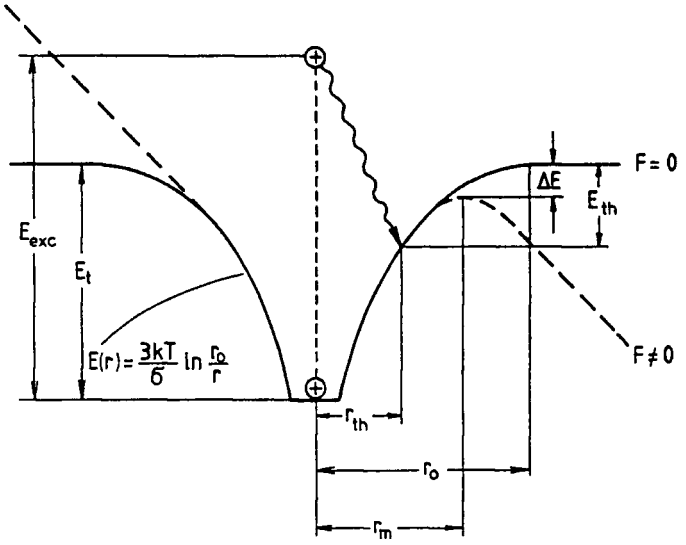

FIGURE 2 Illustration of the carrier (hole) relaxation in a macrotrap in the absence (solid line) and in the presence (dashed line) of an electric field, F. For the thermalization length $r_{th} > r_m$, the release efficiency η (F) = const, for $r_{th} < r_m$, η is a function of F and potential parameters of the macrotrap: $\eta = \eta_o(r_{th}/r_o)^{3/\sigma}\exp(\Delta E/kT)$ (η_o - activationless efficiency, $r_{th} \geq r_m$).

From (3a), (6), (8) and (10)

$$\theta(U) \approx \frac{\eta_o k_{Th} \kappa\tau_{SO}\tau_{TO} k_{ISC} I_0}{4\pi r_o D N_0} \left(\frac{r_{th}}{r_o}\right)^{3/\sigma} \cdot \exp\left(\frac{eUr_o}{kTd}\right) , \tag{11}$$

and (5) yields

$$j \sim (U^2/d^3)\exp\left(\frac{eUr_o}{kTd}\right) \quad \text{and} \quad j \sim I_o \tag{12}$$

for $r_{th} < r_m$ (see Fig. 2).

However, for $r_{th} > r_m$, $\eta = \eta_o$,

$$\theta(U) \approx \frac{\eta_o k_{Th} \kappa\tau_{SO}\tau_{TO} k_{ISC} I_0}{4\pi r_o D N_0} = \text{const} , \tag{13}$$

and

$$j \sim U^2/d^3 \quad \text{and} \quad j \sim I_0 \tag{14}$$

(b) $k_{Th} n_t \tau_{TO} \gg 1$.

From (3b), (4), (6), (8) and (10)

$$\theta(U) \approx \frac{\eta_0 \kappa \tau_{SO} k_{ISC} I_0 e d^2}{6\pi r_0 D N_0 \epsilon \epsilon_0 U} \cdot \left(\frac{r_{th}}{r_0}\right)^{3/\sigma} \cdot \exp\left(\frac{eUr_0}{kTd}\right) , \tag{15}$$

and (5) yields

$$j \sim (U/d) \exp\left(\frac{eUr_0}{kTd}\right) \quad \text{and} \quad j \sim I_0 \tag{16}$$

for $r_{th} < r_m$ (see Fig. 2).

On the other hand, for $r_{th} \geq r_m$, $\eta = \eta_0$,

$$\theta(U) \approx \frac{\eta_0 \kappa \tau_{SO} k_{ISC} I_0 e d^2}{6\pi r_0 D N_0 \epsilon \epsilon_0 U} , \tag{17}$$

and

$$j \sim U/d = F \quad \text{and} \quad j \sim I_0 . \tag{18}$$

High-field region (HFR)

(a) $k_{Th} n_t \tau_{TO} \ll 1$.

From (3a), (6), (9) and (10)

$$\theta(U) \approx \eta_0 \left(\frac{r_{th}}{r_0}\right)^{3/\sigma} \cdot \left(\frac{er_0\sigma}{kT}\right)^{3/\sigma} \cdot \frac{k_{Th} \kappa \tau_{SO} k_{ISC} \tau_{TO} I_0}{4\pi r_0 D N_0} \cdot \left(\frac{U}{d}\right)^{3/\sigma} \tag{19}$$

and (5) yields

$$j \sim U^{3/\sigma+2} / d^{3/\sigma+3} \quad \text{and} \quad j \sim I_0 \tag{20}$$

for $r_{th} < r_m$ (see Fig. 2).

For $r_{th} \geq r_m$, (13) and (14) obey.

(b) $k_{Th} n_t \tau_{TO} \gg 1$.

From (3b), (4), (6), (8) and (10)

$$\theta(U) \approx \eta_0 \left(\frac{r_{th}}{r_0}\right)^{3/\sigma} \cdot \left(\frac{er_0\sigma}{kT}\right)^{3/\sigma} \cdot \frac{e\kappa\tau_{SO}k_{ISC}I_0}{6\pi\epsilon\epsilon_0 r_0 DN_0} \cdot \frac{U^{3/\sigma-1}}{d^{3/\sigma-2}} , \tag{21}$$

and (5) yields

$$j \sim (U/d)^{3/\sigma+1} \quad \text{and} \quad j \sim I_0 \tag{22}$$

for $r_{th} < r_m$ (see Fig. 2).

For $r_{th} \geq r_m$, (17) and (18) obey.

COMPARISON WITH EXPERIMENT

The data of Figure 1 show the agreement of various limiting cases of the model with experiment. The j (F) (d= const) for one of the 78 μm-thick crystals (circles) follows quadratic dependence, suggesting weak triplet exciton quenching by injected holes and thermalization length exceeding position of the potential barrier (case LFR (a)). The HFR (a) case can be excluded since by definition $F < F_{HFR} = 3kT/\sigma er_0 \approx 10^4$V/cm for $\sigma = 1$ and $r_0 = 50$ nm (cf.Refs. 5 and 6). Slightly overlinear dependence in the LFR for the second of the 78 μm-thick crystals (squares) suggests that we are dealing with the strong triplet exciton quenching case with r_{th} shorter than the barrier position r_m (case LFR (b)). A power dependence of $j(F) \sim F^m$ with $m = 3.5$, as for the 94 μm-thick crystal (triangles), is predicted by Eq. (20) for HFR with weak exciton quenching and carrier thermalization within the trap potential well or by Eq. (22) with strong triplet exciton quenching. It would be possible to distinguish these two cases on the basis of measurements of τ_{TO}. A distinct change in shape of the j(F) occurs prior to approaching the value of the dark current at high fields in each case. This would be expected owing to the increased influence of thermal detrapping leading to the inequality opposite to (10) and, consequently, to[5,6]

$$j \approx j_{dark} \sim U^n \quad \text{with} \quad n = 3/\sigma + 2 \tag{23}$$

Note, however, that σ determined from j_{dark} and j are different in general. For the 94 μm-thick crystal, σ_{dark} = 0.45 and σ = 1.2 (see (22)). This situation would be expected for the two-branches macrotrap potential well as observed in solution-grown anthracene crystals from an analysis of SCLC.[5,6] The flat branch of the potential (with high σ) is operative in the LFR (and/or prevailing optical detrapping), and the steep branch (with small σ) determines the HFR thermal detrapping of charge carriers.

CONCLUSION

We have shown that the macrotrap concept for charge carrier trapping[5,6] can be successfully applied to explain photo-enhanced currents (PEC) in anthracene like crystals. The field characteristics of PEC takes different functional shapes dependent on the macrotrap parameters (σ, r_0), the main pathway for exciton decay (spontaneous or quenching by the injected charge), and thermalization length of excited carriers. In contrast to point-trap approach, the macrotrap model allows to explain non quadratic field behaviour of PEC, including the observed power dependence $j \sim F^m$ with m = 1,2 and n > 2 as well as more complex behaviour expressed by a combination of a power and an exponential function of F. The model predicts linear increase of PEC with light intensity.

REFERENCES

1. M. Pope and C.E. Swenberg, Electronic Processes in Organic Crystals, p. 404, Clarendon, Oxford (1982).
2. W. Helfrich, Physics and Chemistry of the Organic Solid State (Edited by D. Fox, M . Labes & A. Weissberger), vol. III, p. 1, Intersci. Publ., New York (1967).
3. H. Bauser and H. H. Ruf, Phys. Stat. Sol., 32, 135 (1969).
4. J. Godlewski and J. Kalinowski, Phys. Stat. Sol. (a) 53, 161 (1979).
5. J. Kalinowski, J. Godlewski and P. Mondalski, Mol. Cryst. Liq. Cryst., 175, 67 (1989).
6. J. Kalinowski, J. Godlewski and P. Mondalski, Proc. Int. Conf. Science and Technology of Defect Control in Semiconductors (Edited by K. Sumino) vol. II, p. 1705, North Holland, Amsterdam (1990).
7. J. Kalinowski, W. Stampor and P.G. Di Marco J. Chem. Phys., 96, 4136 (1992).
8. J. Kalinowski, J. Godlewski, P.G. Di Marco and V. Fattori, Jpn. J. Appl. Phys., 31, 818 (1992).
9. D.R. Wight, I.D. Blenkinshop, W. Harding and B. Hamilton, Phys. Rev. B23, 5495 (1981)